

Electronic Supplementary Material (ESI)

The Achievement of Intrinsic White-Light-Emitting by Hybridization Deformable Haloplumbates with Rigid Luminescent Naphthalene Motif

Xiang-Ling Lin,^a Bin Chen,^a You-Ren Huang,^a Kai-Yue Song,^a Pan-Ke Zhou,^a Lu-Lu
Zong,^a Hao-Hong Li^{*a,b}, Zhi-Rong Chen^{*a,b}

Table Caption:

Table S1 Crystal data and structure refinements for 1-3

Table S2 Selected bond lengths (Å) of 1-3

Table S3 Hydrogen bridging details of 1-3

Figure Caption:

Fig. S1 FT-IR spectra of 1-3

Fig. S2 (a) 1D chain constructed from edge- and face-sharing of PbO₆Cl₂ dodecahedrons; (b) the view of 1D (Pb₄Br₂)⁶⁺ zigzag chain; (c) chelate-bridging coordinated mode of 2,6-ndc²⁻

Fig. S3 1D chains constructed from edge -sharing of PbO₆X₂ (X=Br, I) pentagonal bipyramids for 2 (a) and (b); (c) 3D networks of 2 and 3

Fig. S4 The simulated (red) and experimental (green) PXRD of the crystal 1 (a); 2 (b); 3 (c); UV-Vis spectra of solutions after after filtrating the soaked crystals (d)

Fig. S5 The TGA curves of 1-3 (a); The PXRD of 1 (b) and 2 (c) and 3 (d) before and after chemical treatment

Fig. S6 The UV-Vis absorption spectra of 1-3 (a), Kubelka-Munk plots of 1 (b), 2(c), 3(d)

Fig. S7 Solid-state emission spectra of 2,6-H₂ndc ligand

Fig. S8 The photoluminescence decay curves (black) and the fit plot (red) of 1 (a); 2 (b); 3 (c) at room temperature

Fig. S9 Photoluminescence measured by heating from 303 to 443K (for 1, a), 303 to 423 K (for 2, b) and 303 to 403 K (for 3, c)

Fig. S10 Photoluminescence of bulk crystals and grinded powder for compounds 1 (a), 2 (b), 3 (c) measured at room temperature

Fig. S11 The SEM images of bulk crystals and grinded powder of 1 (a, b), 2 (c, d), 3 (e, f)

Table S1 Crystal data and structure refinements for 1-3

Compound	1	2	3
Empirical formula	C ₅₄ H ₃₈ Cl ₂ N ₂ O ₁₆ Pb ₄	C ₅₂ H ₃₆ Br ₂ N ₂ O ₁₆ Pb ₄	C ₅₂ H ₄₀ I ₂ N ₂ O ₁₆ Pb ₄
Formula weight	1870.61	1933.41	2031.42
Temperature/K	175	175	175
Crystal system	Monoclinic	Monoclinic	Monoclinic
Space group	C2/c	C2/c	C2/c
a/Å	17.500(4)	17.548(3)	17.433(2)
b/Å	23.051(4)	23.128(3)	22.934(3)
c/Å	8.0270(14)	8.0703(12)	7.9945(10)
β/°	116.673(4)	116.872(2)	116.603(2)
Volume/Å ³	2893.4(9)	2921.5(8)	2857.8(6)
Z	2	2	2
D _c /g·cm ⁻³	2.145	2.198	2.361
μ/mm ⁻¹	11.762	12.923	12.894
F(000)	1728	1776.0	1856
Index ranges	-20 ≤ h ≤ 20, -19 ≤ k ≤ 27, -9 ≤ l ≤ 9	-19 ≤ h ≤ 21, -28 ≤ k ≤ 25, -9 ≤ l ≤ 9	-10 ≤ h ≤ 20, -27 ≤ k ≤ 23, -9 ≤ l ≤ 9
Reflections collected	8750	8506	4713
Independent reflections	2485 [R _{int} = 0.0274]	2886 [R _{int} = 0.0240]	2444 [R _{int} = 0.0178]
Reflections, observed	2352	2743	2425
No. of parameters refined	180	174	175
Goodness-of-fit on F ²	1.072	1.120	1.12
Final R indexes [I>=2σ (I)]	R ₁ = 0.0214, wR ₂ = 0.0562	R ₁ = 0.0367, wR ₂ = 0.0955	R ₁ = 0.0621, wR ₂ = 0.1794
Largest diff. peak/hole / e Å ⁻³	1.475, -0.739	1.78, -4.17	2.40, -5.95

Table S2 Selected bond lengths (Å) of 1-3

1					
Pb(1)-O(1)	2.401(4)	Pb(1)-O(2)	2.797(5)	Pb(1)-O(2)#1	2.563(4)
Pb(1)-O(3)	2.532(4)	Pb(1)-O(4)	2.485(4)	Pb(1)-O(4)#3	2.485(4)
Pb(1)-Cl(1)	3.163(10)	Pb(1)-Cl(1)#2	3.186(3)		
O(1)-Pb(1)-O(4)	77.79(13)	O(1)-Pb(1)-O(3)	77.89(15)	O(4)-Pb(1)-O(3)	52.50(13)
O(1)-Pb(1)-O(2)#1	87.04(13)	O(4)-Pb(1)-O(2)#1	73.90(12)	O(3)-Pb(1)-O(2)#1	126.14(12)
O(1)-Pb(1)-Cl(1)	152.11(9)	O(4)-Pb(1)-Cl(1)	74.63(9)	O(3)-Pb(1)-Cl(1)	88.54(10)
O(2)#1-Pb(1)-Cl(1)	81.45(8)				

Symmetry codes: #1 x,-y+1,z-1/2; #2 -x,y,-z-1/2; #3 x,-y+1,z+1/2

2

Pb(1)-O(1)	2.321(15)	Pb(1)-O(2)	2.791(22)	Pb(1)-O(2)#1	2.543(16)
Pb(1)-O(3)	2.537(16)	Pb(1)-O(3)#3	2.837(16)	Pb(1)-O(4)	2.549(16)
Pb(1)-Br(1)	3.2037(8)	Pb(1)-Br(1)#2	3.2374(8)		
O(1)-Pb(1)-O(3)	76.9(6)	O(1)-Pb(1)-O(2)#1	87.7(6)	O(3)-Pb(1)-O(2)#1	72.1(5)
O(1)-Pb(1)-O(4)	77.0(6)	O(3)-Pb(1)-O(4)	54.9(5)	O(2)#1-Pb(1)-O(4)	126.8(5)
O(1)-Pb(1)-Br(1)	151.4(4)	O(3)-Pb(1)-Br(1)	74.6(3)	O(2)#1-Pb(1)-Br(1)	81.3(4)
O(4)-Pb(1)-Br(1)	88.6(4)	O(1)-Pb(1)-Br(1)#2	128.7(4)	O(3)-Pb(1)-Br(1)#2	141.1(4)
O(2)#1-Pb(1)-Br(1)#2	129.1(4)	O(4)-Pb(1)-Br(1)#2	98.4(4)	Br(1)-Pb(1)-Br(1)#2	77.33(2)

Symmetry codes: #1 x,-y+1,z+1/2; #2 -x+1,y,-z+3/2; #3 x,-y+1,z-1/2

3

Pb(1)-O(1)	2.384(9)	Pb(1)-O(2)	2.792(9)	Pb(1)-O(2)#1	2.530(9)
Pb(1)-O(3)	2.512(9)	Pb(1)-O(4)	2.474(9)	Pb(1)-O(4)#3	2.904(10)
Pb(1)-I(1)	3.1520(6)	Pb(1)-I(1)#2	3.1750(6)		
O(1)-Pb(1)-O(4)	78.3(3)	O(1)-Pb(1)-O(3)	77.8(3)	O(4)-Pb(1)-O(3)	52.4(3)
O(1)-Pb(1)-O(2)#1	86.6(3)	O(4)-Pb(1)-O(2)#1	74.0(3)	O(3)-Pb(1)-O(2)#1	126.1(3)
O(1)-Pb(1)-I(1)	152.2(2)	O(4)-Pb(1)-I(1)	74.3(2)	O(3)-Pb(1)-I(1)	89.0(2)
O(2)#1-Pb(1)-I(1)	81.6(2)	O(1)-Pb(1)-I(1)#2	127.5(2)	O(4)-Pb(1)-I(1)#2	140.2(2)
O(3)-Pb(1)-I(1)#2	99.28(19)	O(2)#1-Pb(1)-I(1)#2	129.69(19)		

Symmetry codes: #1 x,-y+1,z-1/2; #2 -x,y,-z+1/2; #3 x,-y+1,z+1/2

Table S3 Hydrogen bridging details of 1-3

Compound	D-H···A	D-H/Å	H···A/Å	D···A/Å	$\angle(D-H\cdots A)^\circ$	Symmetry codes
1	C(6)-H(6)···O(1)	0.93	2.45	2.7664	100	Intra
	C(12)-H(12)···O(2)	0.93	2.44	3.3581	168	x,y,1+z
2	C(8)-H(8)···O(1)	0.95	2.46	3.395(11)	169	x,y,1+z
3	C(7)-H(7)···O(1)	0.93	2.43	3.3428(4)	168	x,y,1+z
	C(11)-H(11)···O(2)	0.93	2.39	2.7206(4)	101	Intra

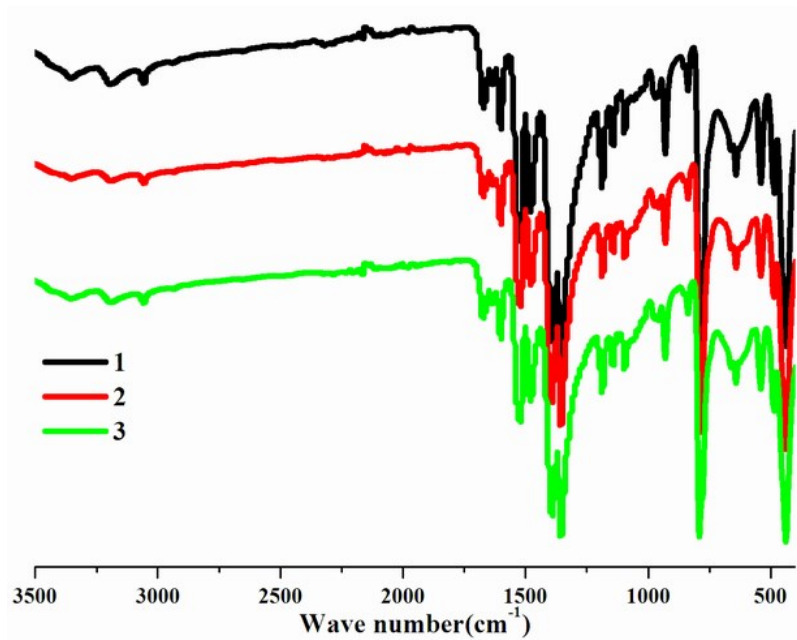


Fig. S1 FT-IR spectra of 1-3

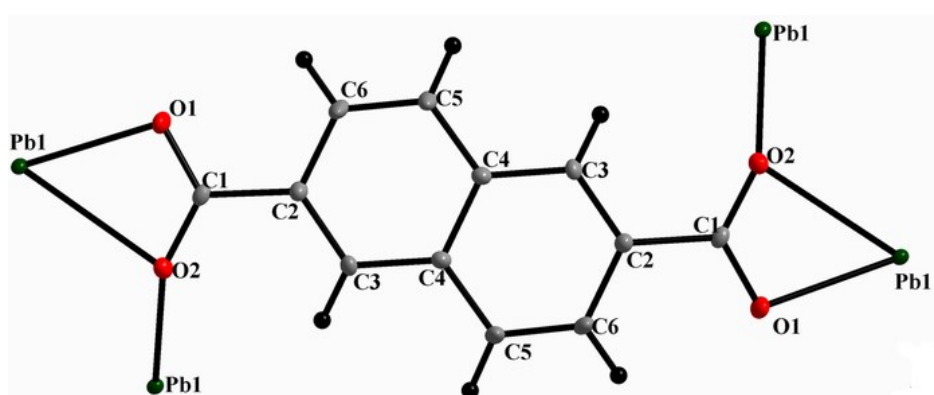
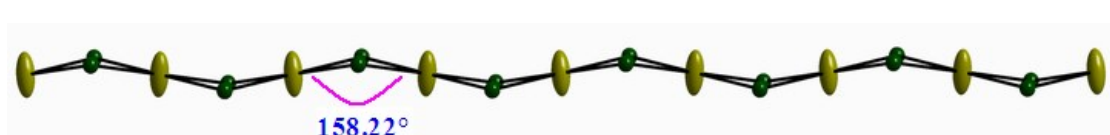
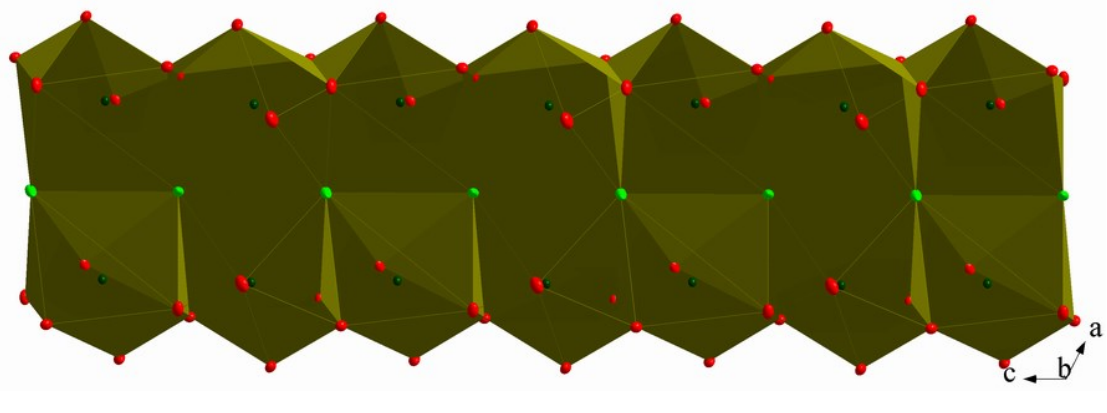


Fig. S2 (a) 1D chain constructed from edge- and face-sharing of PbO_6Cl_2 dodecahedrons; (b) the view of 1D $(\text{Pb}_4\text{Br}_2)^{6+}$ zigzag chain; (c) chelate-bridging coordinated mode of $2,6\text{-ndc}^{2-}$

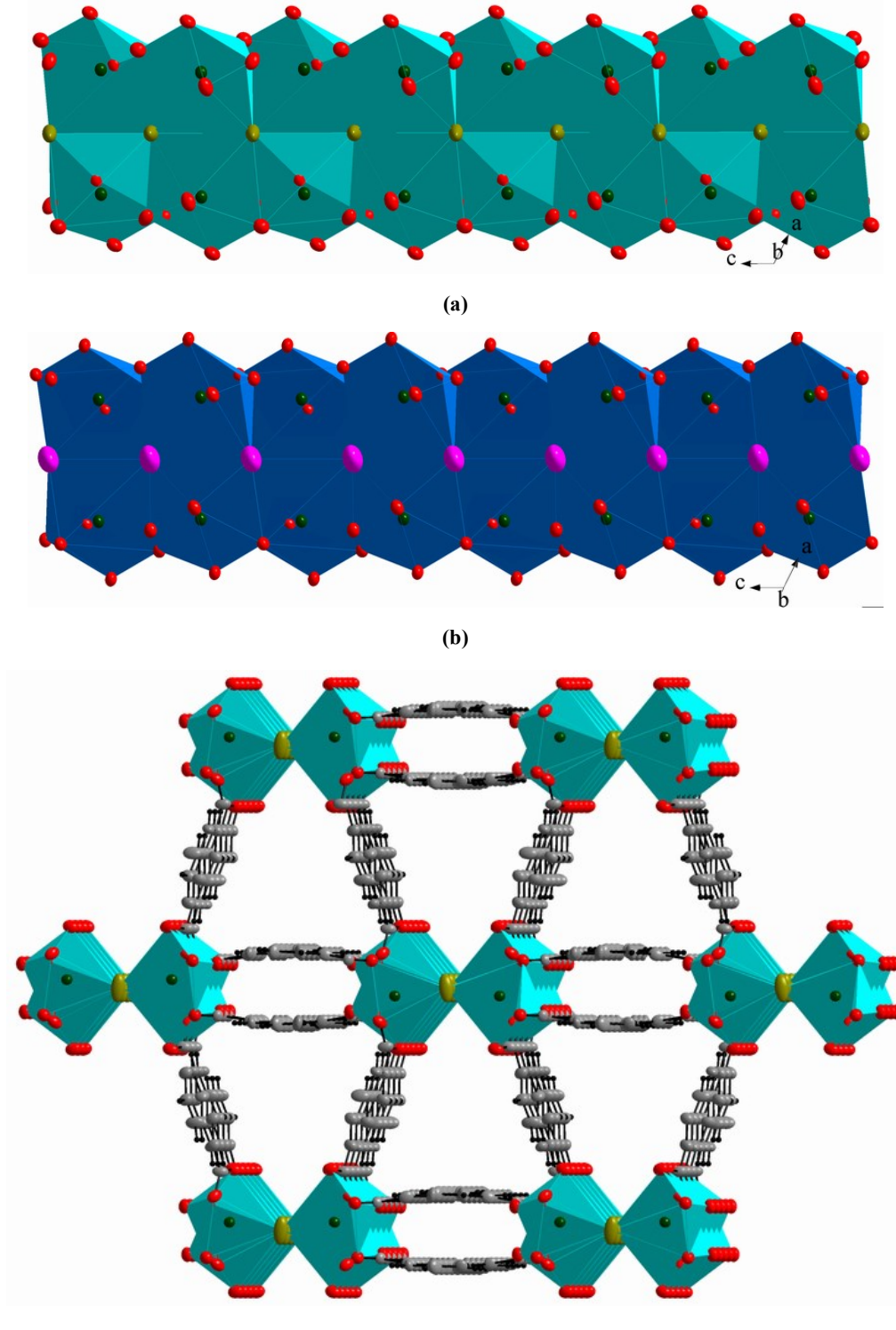
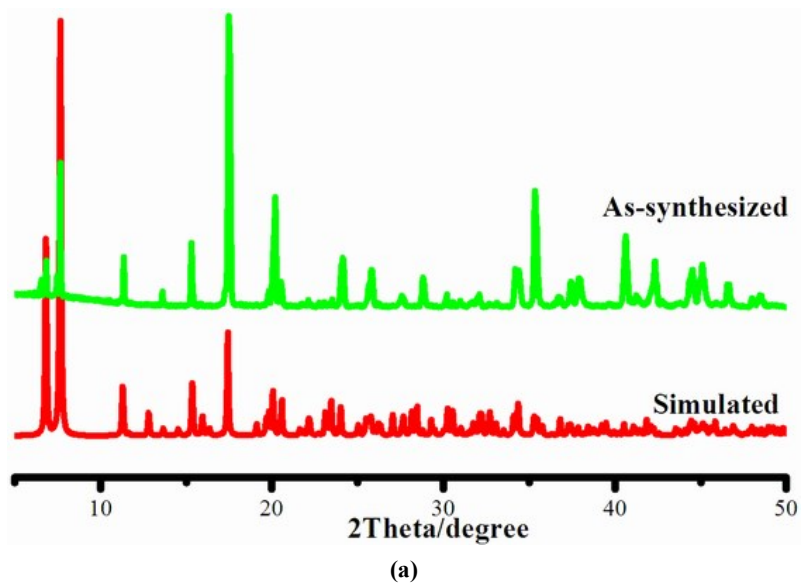
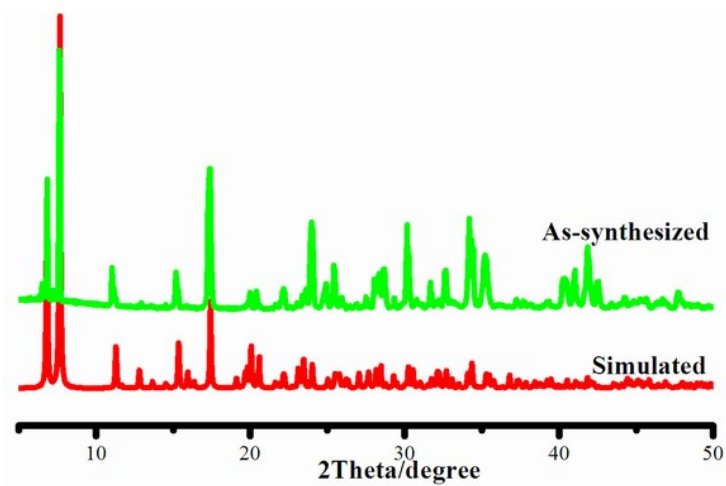


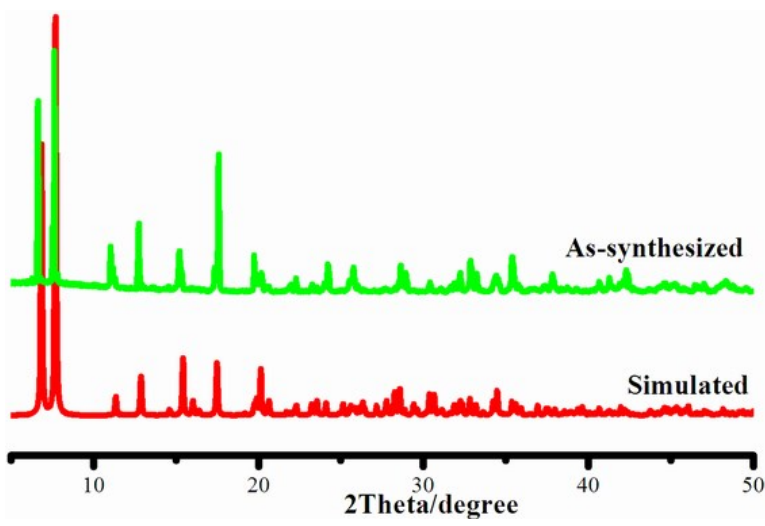
Fig. S3 1D chains constructed from edge -sharing of PbO_6X_2 ($\text{X}=\text{Br}, \text{I}$) pentagonal bipyramids for 2 (a) and (b); (c) 3D networks of 2 and 3



(a)



(b)



(c)

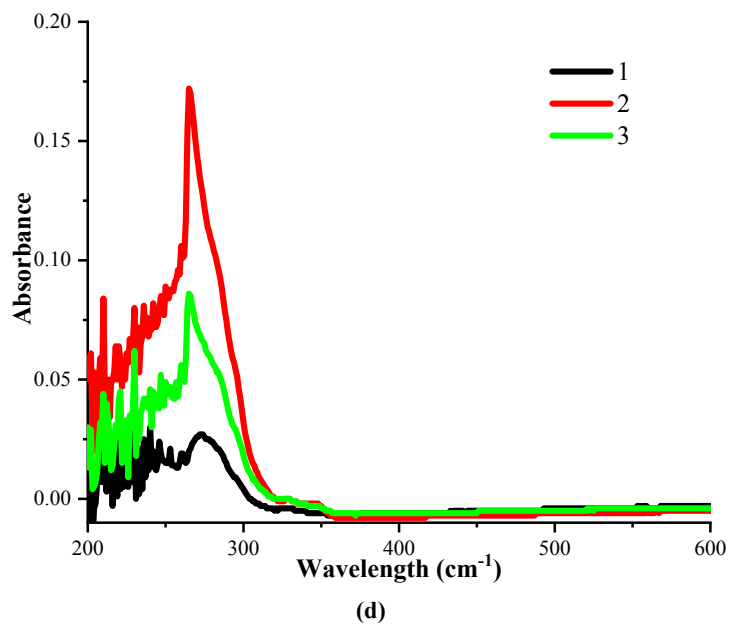


Fig. S4 The simulated (red) and experimental (green) PXRD of the crystal 1 (a); 2 (b); 3 (c); UV-Vis spectra of solutions after after filtrating the soaked crystals (d)

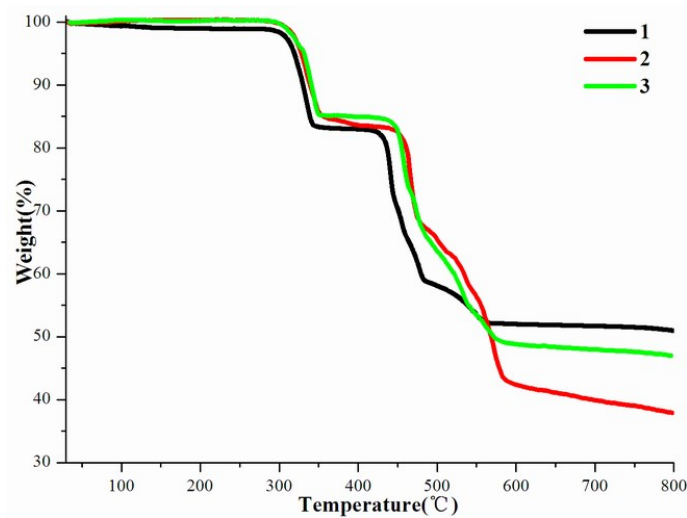
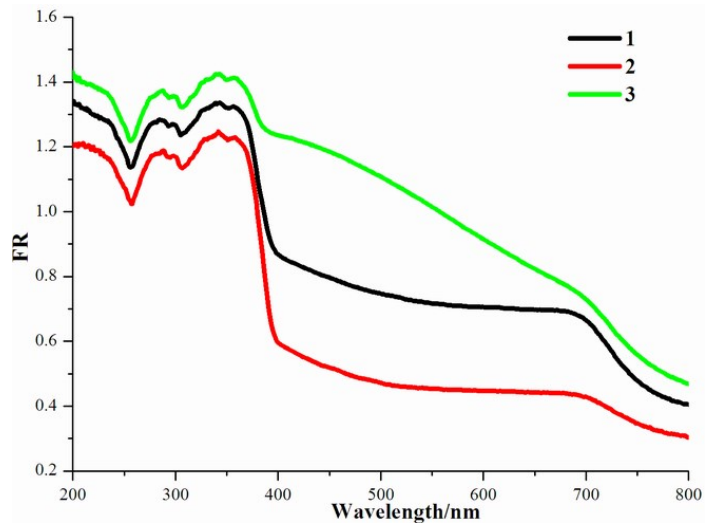
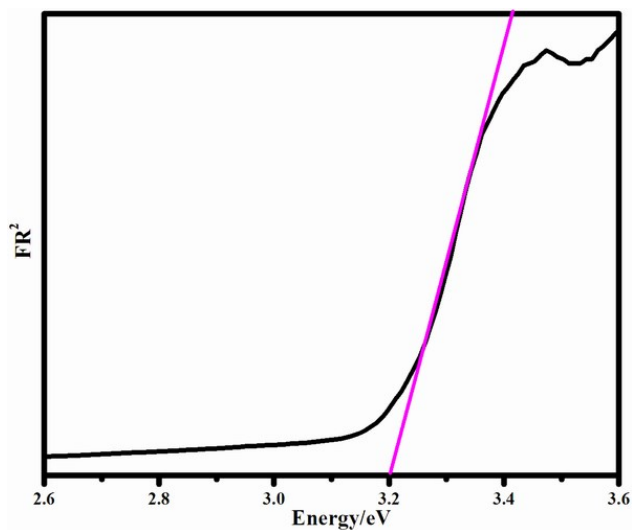


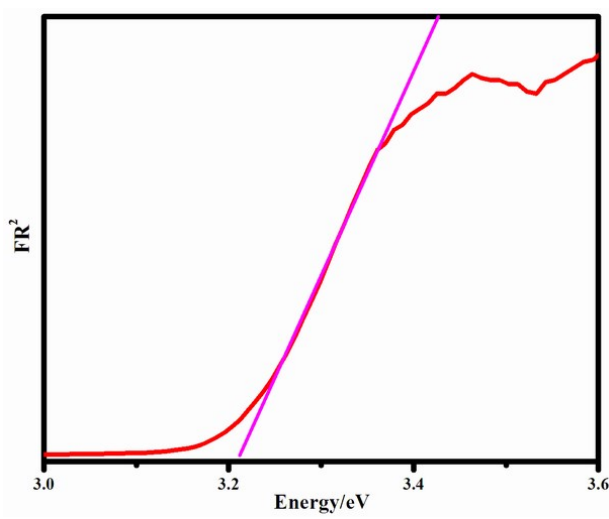
Fig. S5 The TGA curves of 1-3



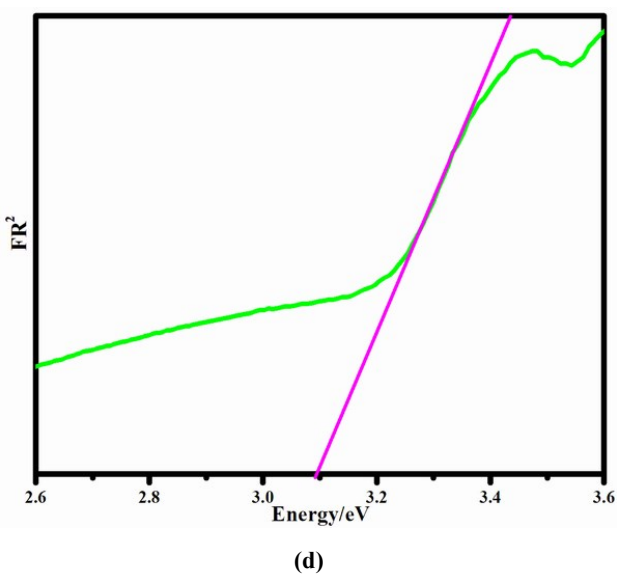
(a)



(b)



(c)



(d)

Fig. S6 The UV-Vis absorption spectra of 1-3 (a), Kubelka-Munk plots of 1 (b), 2(c), 3(d)

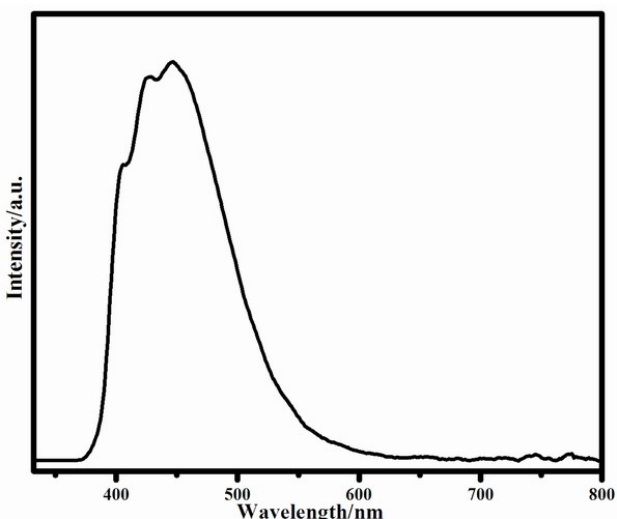
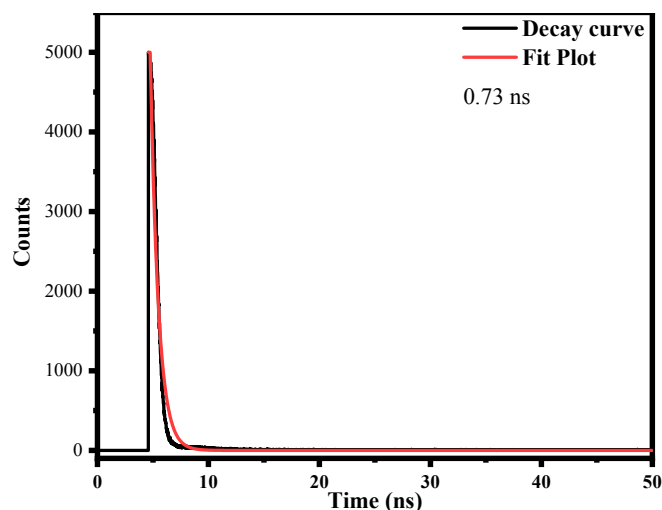
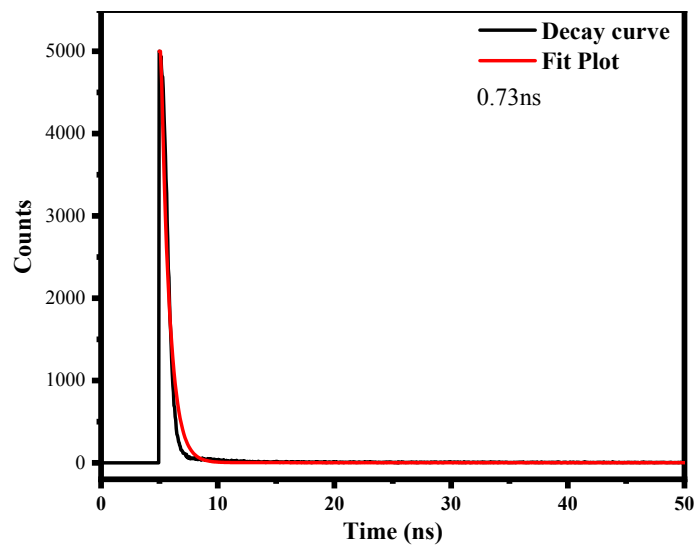


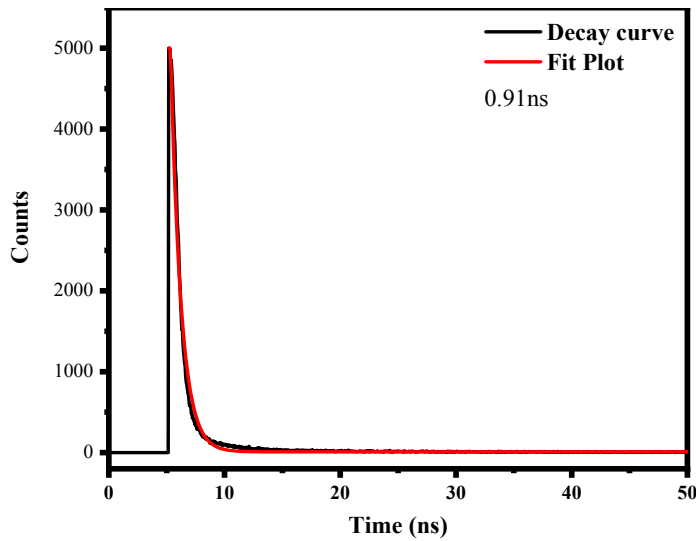
Fig. S7 Solid-state emission spectra of 2,6-H₂ndc ligand



(a)

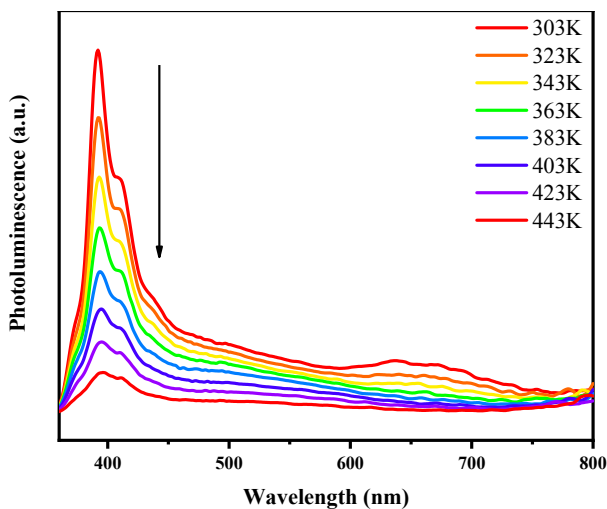


(b)



(c)

Fig. S8 The photoluminescence decay curves (black) and the fit plot (red) of 1 (a); 2 (b); 3 (c) at room temperature



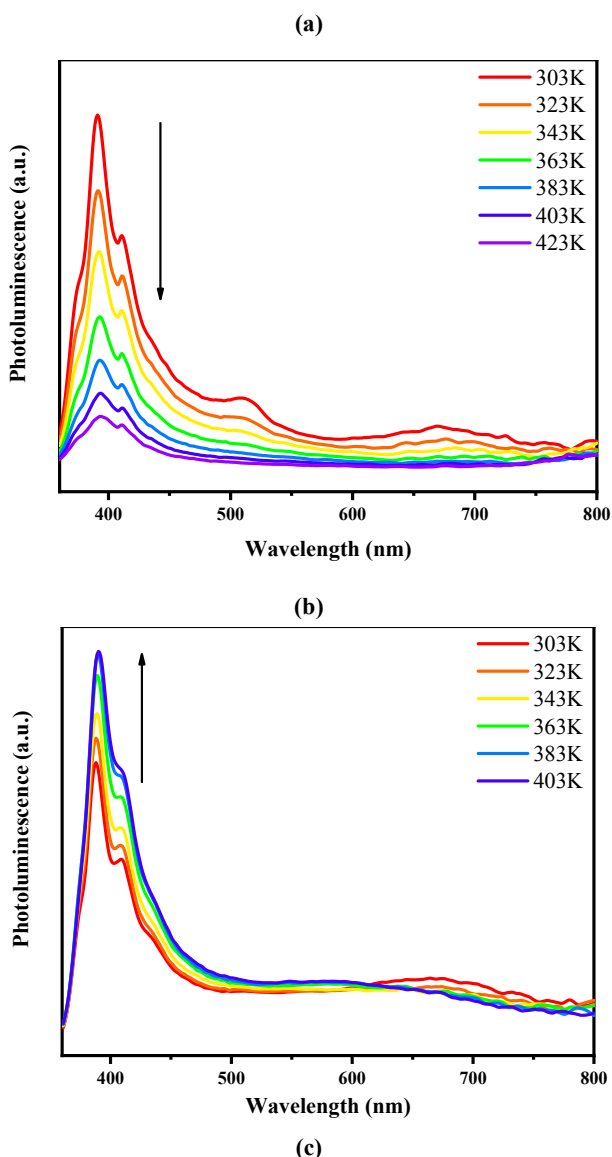
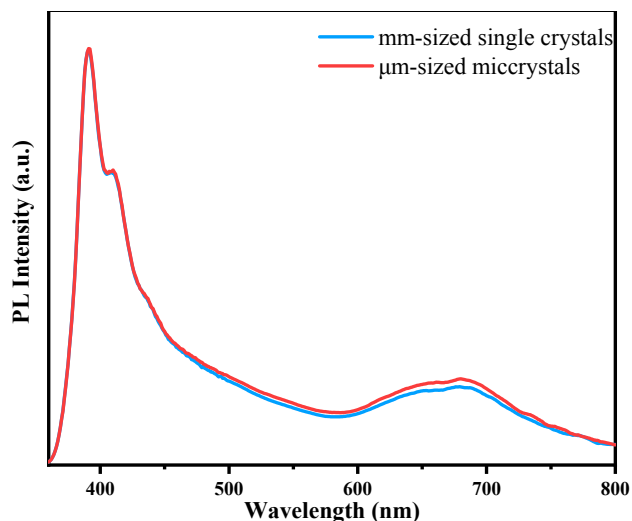
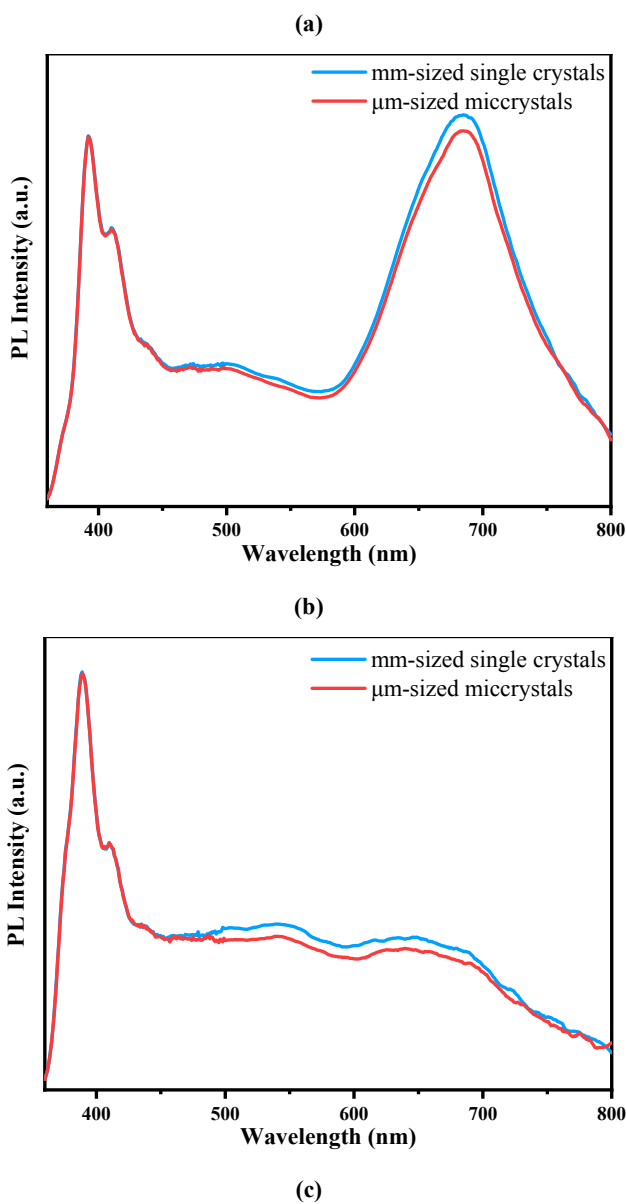


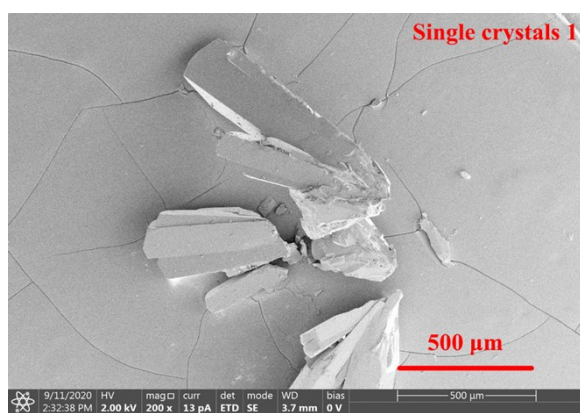
Fig. S9 Photoluminescence measured by heating from 303 to 443K (for 1, a), 303 to 423 K (for 2, b) and 303 to 403 K (for 3, c)



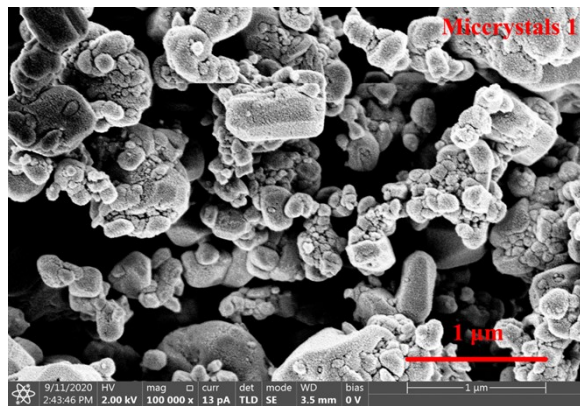


(c)

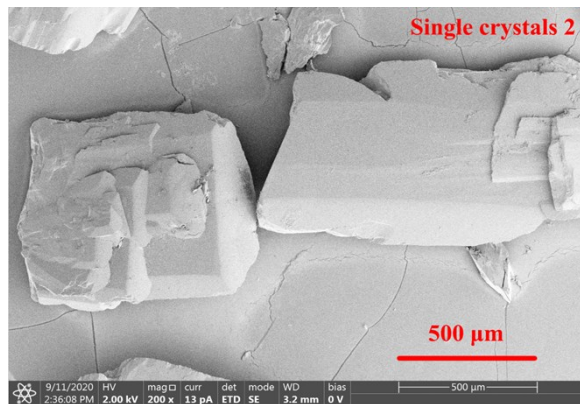
Fig. S10 Photoluminescence of bulk crystals and grinded powder for compounds 1 (a), 2 (b), 3 (c) measured at room temperature



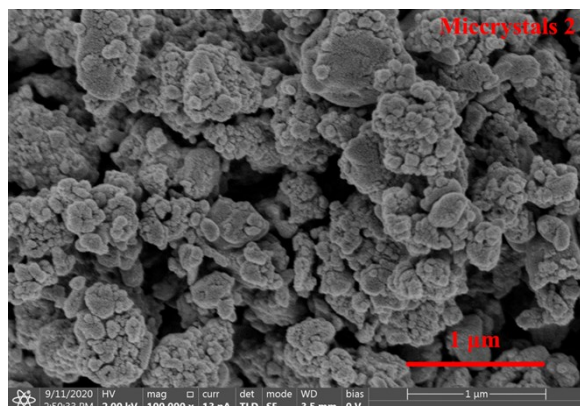
(a)



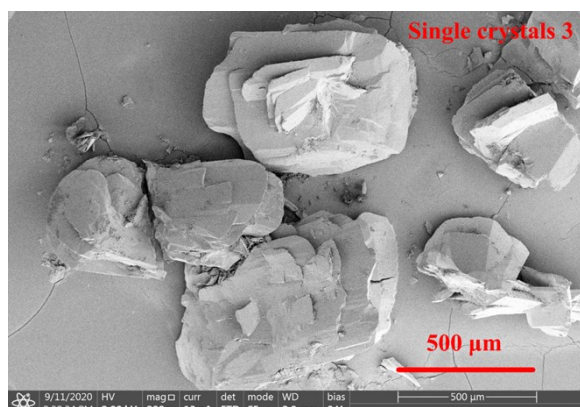
(b)



(c)



(d)



(e)

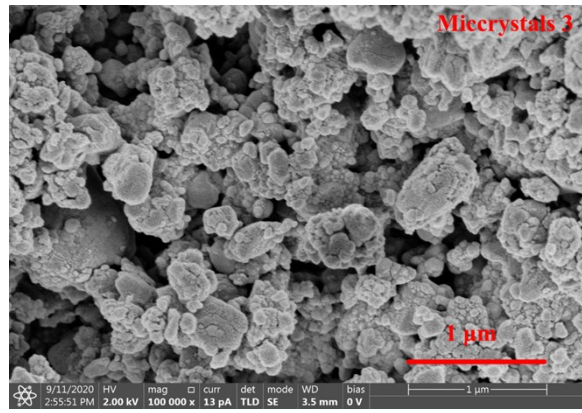


Fig. S11 The SEM images of bulk crystals and grinded powder of 1 (a, b), 2 (c, d), 3 (e, f)